J. Eng. Technol. Sci., Vol. 53, No. 4, 2021, 210411

LSCF-CuO as Promising Cathode for IT SOFC

Ahmad Fuzamy Bin Mohd Abd Fatah, Mohamad Nazri Murat & Noor Ashrina A. Hamid*

School of Chemical Engineering, Engineering Campus, Universiti Sains Malaysia
14300 Nibong Tebal, Malaysia
*E-mail: chrina@usm.my

Highlights:

- The optimal calcination temperature of LSCF-CuO was found to be 700 °C.
- Physical characterizations showed that increasing the calcining temperature resulted in increased particle size.
- The polarization resistance was reduced up to 89% after lowering the calcining and sintering temperature to 700 °C.
- The activation energy of the LSCF-CuO was found to be much lower than that of conventional LSCF.

Abstract. Infiltration of copper oxide towards LSCF was done in order to enhance cathode performance due to superior properties, including high electrical conductivity and high catalytic activity for the oxygen reduction reaction. Samples were synthesized at different temperatures using the sol-gel route. The TGA results showed that LSCF achieved complete perovskite formation when calcined above 600 °C and DTA showed the formation of lattice oxygen at 550 °C. XRD analysis showed no shifted peaks and nano size levels were achieved when samples were calcined at 700 °C and 800 °C. SEM and BET showed similar analysis patterns, where the particle size increased as the calcining temperature was increased. EIS analysis further verified that the polarization resistance of the sample calcined at 700 °C was as small as 0.161 Ω, compared to 1.524 Ω with a calcination temperature of 800 °C. The activation energy of LSCF-CuO was found to be 122.2 kJ/mol, which is much lower than for conventional LSCF.

Keywords: *LSCF-CuO; physical characterization; modified sol-gel method; IT-SOFCs; activation energy.*

1 Introduction

Solid oxide fuel cells (SOFCs) operate based on a thermally activated electrochemical reaction that requires a relatively high operating temperature to promote a redox reaction [1]. There are three major components in a complete fuel cell, i.e. cathode, electrolyte, and anode. Each of them needs to have good chemical compatibility, else fuel cell performance will be negatively affected [2]. One of the major disadvantages of using SOFCs is the high operating temperature

Received January 26th, 2021, Revised February 14th, 2021, Accepted for publication April 16th, 2021.
 ISSN: 2337-5779,
DOI: 10.5614/j.eng.technol.sci.2021.53.4.11

of over 1000 °C. Therefore, the challenge is to develop a material with good performance within an intermediate temperature range for SOFCs (IT-SOFC), which indirectly allows for the reduction of production costs while maintaining the performance level, because the decrease in balance-of-plant complexity is expected to reduce the overall cost of the fuel cell system [3-6].

Fabrication of cathodes via the sol-gel method is generally done by converting the monomer into the sol-gel state, which will then act as precursor for an integrated network. It is expected that the process involves mixing elements at the molecular level since polymerized and chelating agents are introduced into the mixture [7]. One practical method in sol-gel processing is the Pechini approach, where a polymerized agent and a chelating agent are mixed with the element to form a gel to which direct heat is applied to densify the mixture [8]. A suitable transition metal with high oxygen ions for IT-SOFCs is cerium-based electrolyte. Meanwhile, doping of samarium is able to improve the oxide ion conductivity in the electrolyte, which enhances the ion exchange from one side to the other. Furthermore, Sm^{3+} doped ceria has higher ionic conductivity, since samarium has low enthalpy between the doped cation and oxygen vacancy of the host lattice, which as a result of its higher ionic radius compared to cerium eventually leads to excessive oxygen vacancies formation, thus leading to the improvement of ionic conductivity [9]. The density of samarium doped ceria was reported above 90% when the pellet was sintered between 1300 °C and 1500 °C. It showed good density for electrochemical performance evaluation [8].

Mixed ionic-electronic conducting material (MIEC) is a combination of various metal salts that have great chemical compatibility among themselves. An MIEC cathode choice that is commonly applied in intermediate temperature SOFCs is LSCF due to its excellent ionic and electronic conductivities, which are capable of expanding the active sites from the triple boundary phase to the entire cathode surface [10-12]. Currently, conventional LSCF has to be calcined at a high temperature (about 1000 °C) to get good adhesion to the electrolyte in an intermediate temperature range. However, as the temperature increases, the grain size also increases and thus the electro-catalytic activity decreases [8]. Therefore, the addition of another element into the cathode matrix is highly advantageous in order to improve the electrocatalytic activity. Copper oxide is an element that can be composited well with LSCF due to its unique chemical composition, which has good chemical compatibility with most of the elements in transition metals [13-15]. Application of CuO composite toward various types of cathodes has been proved, as it is a good catalyst for chemical reactions and an effective sintering aid of ceramics, as reported in [8]. This is because the catalytic property of cathodes are affected by two possible processes, i.e. the oxygen reduction reaction (ORR) and the diffusion of copper oxide into the LSCF lattice. Therefore, the present study focused on the development of a composite LSCF-

CuO cathode using the well-known sol-gel method and further the electrochemical properties as cathode for IT-SOFCs were evaluated.

2 Methodology

$La_{0.6}Sr_{0.4}Co_{0.2}Fe_{0.8}O_3$- (LSCF) and CuO powder were synthesized using the sol-gel method following the polymerized complex method, which is discussed in [8]. Samarium doped ceria ($Sm_{0.2}C_{0.8}$) powder was pressed at 450 Mpa with a diameter of 13 mm and a thickness of approximately 2 mm. The resulted pellets were sintered at 1300 °C for 6 hours. The slurry cathode was produced via the amalgamation of binder and LSCF-CuO at a ratio of 1:1.5 and was then applied to both sides of the cleaned pellet surface. The resulted pellets were sintered at 800 °C and 700 °C respectively to eliminate excess binder and platinum paste was applied to both sides of the pellet to act as a current collector layer.

The phase composition was characterized using X-ray diffraction (XRD) with Cu Kα radiation from 10 θ to 90 θ for the entire sample with a Bruker AXS diffractometer. The raw data from the XRD analysis was analyzed using Xpert-Highscore Plus. The main LSCF-CuO sample calcined at 800 °C was compared with the literature and with LSCF and CuO samples synthesized at the same temperature. The thermal decomposition behavior of the precursor powder was analyzed using a Pelkin Elmer STA 600 TGA analyzer from room temperature to 900 °C with an airflow rate of 50 cm^3/min and a heating rate of 5 °C /min in air. The microstructure of the LSCF-CuO powder was investigated using a Quanta FEG 650 scanning electron microscope. The acceleration voltage was 15-20kV, using a backscattering electron. The behavior of the microstructure of the sample was defined at 500 nm and 5 µm. The specific surface area and total pore volume of the LSCF-CuO was measured using Brunauer-Emmett-Teller (BET) with an average mass of 0.2 gram per sample.

Electrochemical impedance spectra analysis was conducted on an EIS with a furnace system (model ZIVE SP2). Silver wires were attached to the electrode's surface, which had been coated with platinum paste. The temperature for EIS measurement was varied from 800 °C to 600 °C at the same frequency range (from 0.1 Hz to 1 MHz) with a signal amplitude of 10 mv and 5 mv for each sample. The polarization cell was measured using a type-K thermocouple and recorded on a Digi-Sense digital thermocouple meter (Eutech Instruments). ZMAN 2.4 software (ZIVELAB) was used to fit the experimental data to an equivalent circuit and each was plotted in Sigma Plot software version 11. The analysis was conducted in open air.

3 Results

Thermogravimetric analysis (TGA) was conducted to identify the weight loss of the sample, which signifies the formation of lattice oxygen in the sample. Figure 1 shows the TGA/DTA curves of the weight loss of the precursor sample versus temperature, categorized in three phases. The first phase, between 30 °C to 400 °C, was characterized by the removal of adsorbed water, the decomposition of nitrate and the removal of citric acid. This is because most organic compound decomposes below 400 °C.

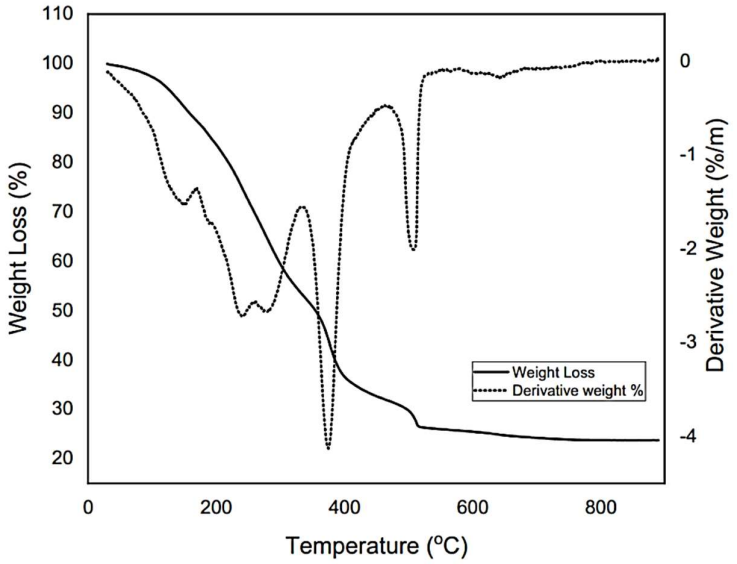

Figure 1 TGA curve of the as-synthesized LSCF in precursor state.

The second phase, which occurred from 400 °C to 600 °C, showed a steeper gradient of weight loss. It shows metal-citrate decomposition, indicating that all the metal salt formed single-phase perovskite. This phase is crucial because the formation of LSCF starts to happen, while the continuous weight loss indicates that LSCF formation continues in this temperature range and the formation of oxygen vacancies also occurs in this phase. The final phase shows a small weight loss related to the formation of oxygen vacancies and the sample started to stabilize, showing that the formation of single-phase perovskite was almost complete. This finding is in agreement with several studies that analyzed LSCF via TGA analysis [8, 16-19]. It was discovered that the optimal calcining temperature was 700 °C, since the DTA curve showed stabilization of the sample after being fired at 700 °C. The results also showed that phase the LSCF lost

76.27% of its weight, from which it can be concluded that the phase purity plays a role in improving the formation of oxygen vacancies. A possible explanation for this is that as the formation of oxygen vacancies increase, the number of pores will increase and the active surface area will also increase. Thus, more oxygen reduction reactions (ORR) will be produced, resulting in an increase of the electrical conductivity.

The result of the XRD analysis of LSCF-CuO with the respective calcination temperatures is shown in Figure 2. The LSCF structure was defined using the comparison and analysis method discussed previously. Figure 2 shows that the LSCF-CuO was able to achieve a single-phase perovskite, since no major shifted peaks were detected. This is because the optimal calcination temperature for LSCF-CuO is usually 700 °C, based on the TGA analysis beforehand, so a comparison was made between the samples and the literature provided precise data for phase comparison. Based on the XRD analysis, all peaks were defined as single-phase perovskite. The LSCF peak showed that it was shifted toward a high angle, indicating the inter-diffusion of La^{+} ions in the LSCF. All peaks were identified as LSCF and CuO. Similar findings were presented in several other articles that conducted XRD analysis towards LSCF, indicating that the highest intensity was achieved at 2θ and between 30° and 40° [20-23].

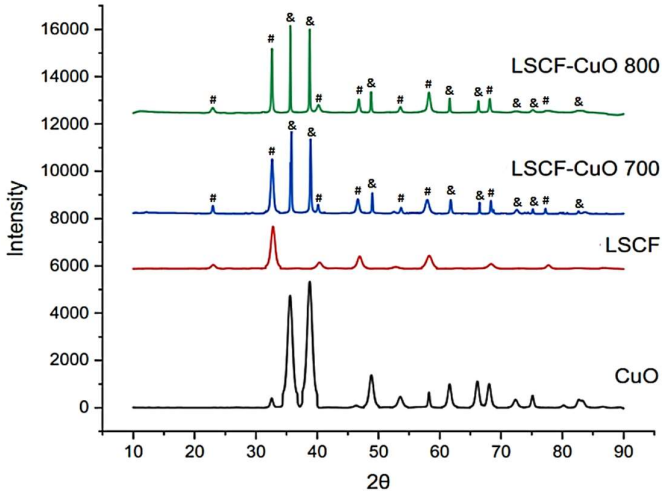

Figure 2 XRD patterns of LSCF, CuO and LSCF-CuO at different calcination temperatures.

A previous study revealed that the addition of CuO was able to reduce the required calcination temperature from 800 °C to 700 °C due to the infiltration on

the B-site of the perovskite [8]. The XRD results from the LSCF-CuO were compared by their respective temperatures. Calculation from the Scherrer equation in Table 1 revealed that the crystalline size of LSCF-CuO calcined at 700 °C was 68.01 nm, while the conventional calcining temperature was found to be around 90.49 nm. This finding provides evidence that LSCF-CuO can maintain a perovskite structure even when it has been calcined at a temperature as low as 700 °C, because temperature is one of the major factors determining cathode performance.

Further characterization was conducted to identify the particle size and contact area between the LSCF-CuO and the SDC. Figure 3 depicts the average particle size estimated using SEM analysis for sol-gel samples on the electrolyte surface while being sintered at the respective temperatures. It can be said that as the temperature increases, the particle size also increases due to grain growth, which is in line with the calculation from the Scherrer equation. A higher sintering temperature produces agglomerations, leading to particles in bulk form while a lower sintering temperature produces a smaller grain size. This is because as the sintering process continues at the higher temperature, the individual powder particles completely lose their identity and grain boundaries, and then move across prior particle boundaries [24]. This facilitates the movement of atoms or molecules through the mechanism of mass transport, which may be lattice diffusion, surface diffusion or evaporation-condensation and results in grain growth, which has a detrimental effect on the properties of the material [25]. As a result, the polarization resistance may be increased due to the increased particle size.

Further investigation was conducted on a cross-sectional image of the pellet to observe the layer of the LSCF-CuO and SDC electrolyte. It showed that the sample had a good contact area even after calcination at lower temperatures. Figure 3(c) shows the SEM image layer of the LSCF-CuO and the SDC electrolyte after being examined by EIS. It can be seen that the LSCF-CuO and the SDC had a good contact area with no delamination detected after sintering of the sample. A high sintering temperature is needed to promote a good contact area between the cathode and the electrolyte so that the electron transfer can be improved. However, high sintering temperatures can cause the particle size of the cathode to increase, subsequently increasing the polarization resistance. Based on this, sintering at 700 °C is enough to promote a good contact area with the electrolyte and produce a good result in terms of polarization resistance.

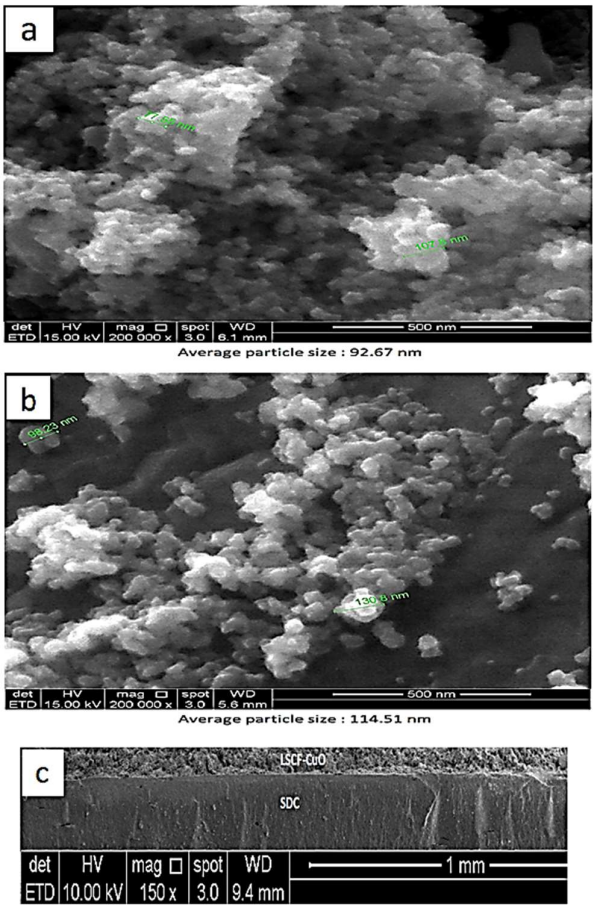

Figure 3 SEM micrographs of the LSCF-CuO (a) calcined at 700 °C, (b) calcined at 800 °C, (c) cross-sectional pellet consisting of LSCF-CuO and SDC.

Table 1 Comparison of the properties of the As-synthesized powders processed at different calcination temperatures.

Calcining temperature (°C)	Scherrer equation (nm)	Specific surface area (m^3/g)	Mean BET-based size (nm)	Particle size from FESEM (nm)
700	68.017	8.158	124.424	92.67
800	90.499	4.172	234.075	114.51

The specific surface area and total pore volume of the LSCF-CuO samples were identified through BET analysis. Table 1 shows a comparison between the

theoretical crystalline size, the theoretical particle size, and the actual particle size calculated based on XRD, BET, and FESEM. This calculation from theoretical and actual data suggests that the LSCF-CuO particles reached a nanosize level.

The specific surface area shows that as the temperature increased, the specific area decreased. This effect can be explained by the fact that when the temperature increases, the particle size also increases due to the grain size increment. Therefore, it was concluded that LSCF-CuO with a small grain size and a high specific surface area was achieved at a temperature of 700 °C via the sol gel method. However, for the preparation of powder size for a slurry-type cathode, a temperature higher than 700 °C is needed to ensure a good contact layer between the cathode and the electrolyte. BET analysis in a previous article showed that both samples passed the porosity range where both had 40% to 20% porosity and since the particle size decreased, the amount of pores inside the sample increased [8]. Therefore, more active contact areas were produced with increased ORR activity.

A further experiment was conducted to measure the polarization resistance of the LSCF-CuO, as shown in Figure 4(d). An equivalent circuit and fitting parameters were generated with the ZMAN software and the parameters were determined as L_s, R_s, R_1, Q_1, indicating the inductance attributed to the silver current-voltage probes or high-frequency phase shift of the EIS equipment. R_s was categorized as R_Ω, which represents the electrolyte resistance and the silver-wire connection resistance. Meanwhile, R_1 and Q_1 represent the low-frequency arc, and R represents the resistance in the frequency region, while Q represents the arc resistance constant phase element (CPE) of the respective frequency regions. Based on the data fitted by the ZMAN software, a new line was produced. The value of R^2 was observed when all the resulted data approached a value of 1. This shows that the fitted value was almost identical to the raw data when the value of R^2 approached a value of 1. All values in the capacitance range from 10^{-4} F to 10^{-3} F were signified as chemical capacitance, while charge transfer and oxygen diffusion were referred to the cathode material and microstructure [26].

Figures 4(a) and (b) depict the performance of the LSCF-CuO for different sintering temperatures towards electrochemical performance at 700 °C. Overall, the LSCF-CuO calcined and sintered at 700 °C provided better results compared to that calcined and sintered at 800 °C. This result is in good agreement with Ref. [26]. The polarisation resistance and area-specific resistance were calculated based on the electrochemical impedance graph. The polarization resistance of the sample that was sintered at 700 °C, shown in Figure 4(a), revealed quite small polarization resistance compare to the sample that was sintered at 800 °C shown in Figure 4(b). These results correspond with the physical characterizations and

this could explain that reducing the calcining temperature caused the particle size to decrease due to the properties of metal.

Further investigation of the addition of copper oxide towards the cathode surface found that the polarisation resistance of the LSCF-CuO was smaller than that of conventional LSCF, as illustrated in Figure 4(c). The value of the activation energy proved that the addition of CuO did indeed act as a synergistic catalyst, since the activation from pure LSCF was reduced. A possible explanation of this phenomenon is that the addition of CuO towards an MIEC type cathode can improve the electrochemical performance by increasing the electro-catalytic activity of the cathode. This shows that the connection between the grains was better in the LSCF-CuO composite cathode, thus improving the charge transfer.

It has been reported that the optimal calcining temperature for LSCF is usually 900 °C. However, a comparison needed to be made between LSCF-CuO and LSCF. Therefore, it was decided to do the calcination and sintering at 800 °C. In a further review, the addition of CuO was able assist in increasing the surface energy of the cathode and the grain boundary speed movement, which resulted in a reduction of the optimal calcining temperature. It has also been reported elsewhere that the addition of CuO in the context of SOFCs was able to perform stable operation for a longer time [27].

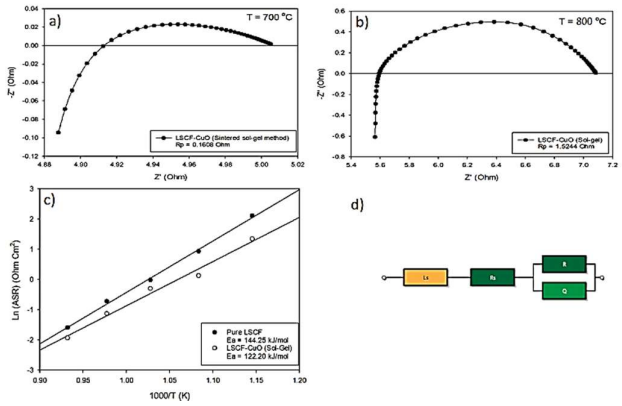

Figure 4 (a) Polarization resistance of LSCF-CuO calcined and sintered at 700 °C, (b) polarization resistance of LSCF-CuO calcined and sintered at 800 °C, (c) comparison of activation energy between LSCF-CuO and conventional LSCF synthesized at 800 °C, (d) schematic diagram of equivalent fitting in ZMAN software.

4 Conclusion

Infiltration of copper oxide towards LSCF was found capable of improving the electrocatalytic activity of a cathode. Moreover, the copper oxide was also proved to have good chemical compatibility with LSCF, as indicated by the characterization results. The effect of the calcining temperature toward the electrochemical performance was evaluated and it was found that reducing the calcining temperature will improve the EIS result. A possible explanation is that as the reducing temperature decreases, the particle size in the cathode decreases due to the properties of metal. In order to improve the cathode, CuO infiltration was implemented and the results showed that CuO infiltration did indeed improve the cathode by providing more and enhanced electrocatalytic activity, as shown by the activation energy and the grain boundary, which subsequently improved the electron transfer inside the electrode.

Acknowledgments

This work was financially supported by the Ministry of Science, Technology & Innovation (MOSTI) Malaysia under Fundamental Research Grant Scheme Malaysia 203 / PJKIMIA / 6071343.

References

[1] Irshad, M., *Evaluation Of Bazr0.8X0.2 (X= Y, Gd, Sm) Proton Conducting Electrolytes Sintered at Low Temperature for IT-SOFC Synthesized by Cost Effective Combustion Method*, J. Alloys Compd., **815**, 2020. DOI: 10.1016/j.jallcom.2019.152389.

[2] Baharuddin, N.A., Muchtar, A. & Somalu, M.R., *Short Review on Cobalt-Free Cathodes for Solid Oxide Fuel Cells*, Int. J. Hydrogen Energy, **42**(14), pp. 9149-9155, 2017. DOI: 10.1016/j.ijhydene.2016.04.097.

[3] Wasajja, H., Lindeboom, R.E.F., van Lier, J.B. & Aravind, P.V., *Techno-Economic Review of Biogas Cleaning Technologies for Small Scale Off-Grid Solid Oxide Fuel Cell Applications*, Fuel Process. Technol., **197**, 106215, 2020. DOI: 10.1016/j.fuproc.2019.106215.

[4] Saadabadi, S.A., Thallam Thattai, A., Fan, L., Lindeboom, R.E.F., Spanjers, H. & Aravind, P.V., *Solid Oxide Fuel Cells Fuelled with Biogas: Potential and Constraints*, Renew. Energy, **134**, pp. 194-214, 2019. DOI: 10.1016/j.renene.2018.11.028.

[5] Fan, L., Zhu, B., Su, P.C. & He, C., *Nanomaterials and Technologies for Low Temperature Solid Oxide Fuel Cells: Recent Advances*, Challenges and Opportunities, Nano Energy, **45**(October 2017), pp. 148-176, 2018. DOI: 10.1016/j.nanoen.2017.12.044.

[6] Abdelkareem, M.A., Tanveer, W.H., Sayed, E.T., Assad, M.E.H., Allagui, A. & Cha, S.W., *On The Technical Challenges Affecting the Performance of Direct Internal Reforming Biogas Solid Oxide Fuel Cells*, Renew. Sustain. Energy Rev., **101**, June 2018, pp. 361-375, 2019. DOI: 10.1016/j.rser.2018.10.025.

[7] Batool, R., *Structural and Electrochemical Study of Ba0.15Cu0.15Ni0.10Zn0.60 Oxide Anode for Low Temperature Solid Oxide Fuel Cell*, J. Alloys Compd., **780**, pp. 653-659, 2019. DOI: 10.1016/j.jallcom.2018.11.392.

[8] Mohd Abd Fatah, A.F. & Hamid, N.A., *Physical and Chemical Properties of LSCF-CuO as Potential Cathode for Intermediate Temperature Solid Oxide Fuel Cell (IT-SOFC)*, Malaysian J. Fundam. Appl. Sci., **14**(3), pp. 391-396, 2018. DOI: 10.11113/mjfas.v14n3.1220.

[9] Acharya, S.A., Gaikwad, V.M., Souza, S.W.D. & Barman, S.R., *Gd/Sm Dopant-Modified Oxidation State and Defect Generation in Nano-Ceria*, Solid State Ionics, **260**, pp. 21-29, 2014. DOI: 10.1016/j.ssi.2014.03.008.

[10] Liao, M.W., Lin, T.N., Kao, W.X., Yeh, C.Y., Chen, Y.M. & Kuo, H.Y., *Composite Mixed Ionic-Electronic Conducting Ceramic for Intermediate Temperature Oxygen Transport Membrane*, Ceram. Int., **43**(May), pp. S628-S632, 2017. DOI: 10.1016/j.ceramint.2017.05.222.

[11] Laurencin, J., *Reactive Mechanisms of LSCF Single-Phase and LSCF-CGO Composite Electrodes Operated in Anodic and Cathodic* Polarisations, Electrochim. Acta, **174**, pp. 1299-1316, 2015. DOI: 10.1016/ j.electacta.2015.06.080.

[12] Sailah, A., *Fabrication of Lanthanum-based Perovskites Membranes on Porous Alumina Hollow Fi Bre (AHF) Substrates for Oxygen Enrichment*, Ceram. Int., **45**(10), pp. 13086-13093, 2019. DOI: 10.1016/j.ceramint. 2019.03.242.

[13] Baqer, A.A., *Synthesis and Characterization of Binary (Cuo)0.6(Ceo2)0.4 Nanoparticles Via A Simple Heat Treatment Method*, Results Phys., **9**, pp. 471-478, 2018. DOI: 10.1016/j.rinp.2018.02.079.

[14] Xu, C., Hao, X., Gao, M., Su, H. & Zeng, S., *Important Properties Associated with Catalytic Performance Over Three-Dimensionally Ordered Macroporous Ceo2-Cuo Catalysts*, Catal. Commun., **73**, pp. 113-117, 2016. DOI: 10.1016/j.catcom.2015.10.025.

[15] Nicollet, C., *Gadolinium Doped Ceria Interlayers for Solid Oxide Fuel Cells Cathodes: Enhanced Reactivity with Sintering Aids (Li, Cu, Zn), and Improved Densification by Infiltration*, J. Power Sources, **372**, no. November, pp. 157-165, 2017. DOI: 10.1016/j.jpowsour.2017.10.064.

[16] Guo, S., Puleo, F., Wang, L., Wu, W. & Liotta, L.F., *La0.6Sr0.4Co0.2Fe0.79M0.01O3−δ (M = Ni, Pd) perovskites synthesized by Citrate-EDTA method: Oxygen Vacancies Effect on Electrochemical*

Properties, Adv. Powder Technol., **29**(11), pp. 2804-2812, 2018. DOI: 10.1016/j.apt.2018.07.029.

[17] Ayodele, B.V., Bin Mohd Yassin, M.Y., Naim, R. & Abdullah, S., *Hydrogen Production By Thermo-Catalytic Conversion of Methane Over Lanthanum Strontium Cobalt Ferrite (LSCF) and Aal2o3 Supported Ni Catalysts*, J. Energy Inst., **92**(4), pp. 892-903, 2019. DOI: 10.1016/j.joei.2018.07.014.

[18] Rafique, A., *Multioxide Phase-Based Nanocomposite Electrolyte (M@SDC where M= Zn2+/ Ba2+/ La3+/Zr2+ /Al3+) Materials*, Ceram. Int., no. October, pp. 1-7, 2019. DOI: 10.1016/j.ceramint.2019.11.183.

[19] Paymooni, K., Doroodchi, E. & Moghtaderi, B., *Oxygen Adsorption and Desorption Characteristics of LSCF5582 Membranes for Oxygen Separation Applications*, Adv. Powder Technol., **28**(6), pp. 1531-1539, 2017. DOI: 10.1016/j.apt.2017.03.024.

[20] Jamale, A.P., Bhosale, C.H. & Jadhav, L.D*., Electrochemical Behavior of LSCF/GDC Interface in Symmetric Cell: An Application in Solid Oxide Fuel Cells*, J. Alloys Compd., **623**, pp. 136-139, 2015. DOI: 10.1016/j.jallcom.2014.10.122.

[21] Nadeem, M., Hu, B. & Xia, C*., Effect of NiO Addition on Oxygen Reduction Reaction at Lanthanum Strontium Cobalt Ferrite Cathode for Solid Oxide Fuel Cell*, Int. J. Hydrogen Energy, **43**(16), pp. 8079-8087, 2018. DOI: 10.1016/j.ijhydene.2018.03.053.

[22] Muhammed Ali, S.A., Anwar, M., Ashikin, N., Muchtar, A. & Somalu, M.R., *Influence of Oxygen Ion Enrichment on Optical, Mechanical, and Electrical Properties of LSCF Perovskite Nanocomposite*, Ceram. Int., **44**(9), pp. 10433-10442, 2018. DOI: 10.1016/j.ceramint.2018.03.060.

[23] Zhang, L., Hong, T., Li, Y. & Xia, C., *CaO effect on the Electrochemical Performance of Lanthanum Strontium Cobalt Ferrite Cathode for Intermediate-Temperature Solid Oxide Fuel Cell*, Int. J. Hydrogen Energy, **42**(27), pp. 17242-17250, 2017. DOI: 10.1016/j.ijhydene.2017.05.207.

[24] Kim, Y.M., Baek, S.W., Bae, J. & Yoo, Y.S., *Effect of Calcination Temperature on Electrochemical Properties of Cathodes for Solid Oxide Fuel Cells*, Solid State Ionics, **192**(1), pp. 595-598, 2011. DOI: 10.1016/j.ssi.2010.09.014.

[25] Xu, H., Zhang, H. & Chu, A., *An investigation of Oxygen Reduction Mechanism in Nano-Sized LSCF-SDC Composite Cathodes*, Int. J. Hydrogen Energy, **41**(47), pp. 22415-22421, 2016. DOI: 10.1016/j.ijhydene.2016.09.153.

[26] Özden Çelikbilek, Siebert, E., Jauffrès, D., Martin, C.L. & Djurado, E., *Influence of Sintering Temperature on Morphology and Electrochemical Performance of LSCF/GDC Composite Films as Efficient Cathode for SOFC*, Electrochim. Acta, **246**, pp. 1248-1258, 2017. DOI: 10.1016/j.electacta.2017.06.070.

[27] Raju K. & Yoon, D., *Reactive Air Brazing of GDC-LSCF Ceramics Using Ag-10 wt% CuO Paste for Oxygen Transport Membrane Applications GDC-LSCF GDC-LSCF Filler*, Ceram. Int., **42**(14), pp. 16392-16395, 2016. DOI: 10.1016/j.ceramint.2016.07.042.